Title
Collagen fiber crimping following in vivo UVA-induced corneal crosslinking

Journal
Experimental Eye Research, 177(8)

ISSN
0014-4835

Authors
Bradford, Samantha M
Mikula, Eric R
Juhasz, Tibor
et al.

Publication Date
2018-12-01

DOI
10.1016/j.exer.2018.08.009

Peer reviewed

HHS Public Access

Author manuscript

Exp Eye Res. Author manuscript; available in PMC 2019 December 15.

Published in final edited form as:

Exp Eye Res. 2018 December ; 177: 173–180. doi:10.1016/j.exer.2018.08.009.

Collagen fiber crimping following *in vivo* UVA-induced corneal crosslinking

Samantha M. Bradford[a], **Eric R. Mikula**[b], **Tibor Juhasz**[a,b], **Donald J. Brown**[b], **James V. Jester**[a,b,*]

[a]Biomedical Engineering, University of California, Irvine, Irvine, CA, United States

[b]Ophthalmology, University of California, Irvine, Irvine, CA, United States

Abstract

The purpose of this study was to measure collagen fiber crimping (CFC) using nonlinear optical imaging of second harmonic generated (SHG) signals to determine the effects of UVA-riboflavin induced corneal collagen crosslinking (UVA CXL) on collagen structure. Two groups, four rabbits each, were treated in the right eye with standard UVA CXL. In vivo confocal microscopy was performed at 1, 2, and 4 weeks after treatment for the first group and up to three months for the second group to measure epithelial/stromal thickness and corneal haze during recovery. Rabbits were sacrificed at one and three months, respectively, and their corneas fixed under pressure. Regions of crosslinking were identified by the presence of collagen autofluorescence (CAF) and then collagen structure was imaged using SHG microscopy. The degree of CFC was determined by measuring the percentage difference between the length of the collagen fiber and the linear distance traveled. CFC was measured in the central anterior and posterior CXL region, the peripheral non-crosslinked region in the same cornea, and the central cornea of the non-crosslinked contralateral eye. No change in corneal thickness was detected after one month, however the stromal thickness surpassed its original baseline thickness at three months by 25.9 μm. Corneal haze peaked at one month and then began to clear. Increased CAF was detected in all CXL corneas, localized to the anterior stroma and extending to 42.4 ± 3.4% and 47.7 ± 7.6% of the corneal thickness at one and three months. There was a significant ($P < 0.05$) reduction in CFC in the CAF region in all eyes averaging 1.007 ± 0.006 and 1.009 ± 0.005 in one and three month samples compared to 1.017 ± 0.04 and 1.016 ± 0.06 for controls. These results indicate that there is a significant reduction in collagen crimping following UVA CXL of approximately 1%. One possible explanation for this loss of crimping could be shortening of the collagen fibers over the CXL region.

Keywords

Corneal crosslinking; Keratoconus; Corneal imaging; Corneal collagen

*Corresponding author. Biomedical Engineering, University of California, Irvine, Irvine, CA, United States. jjester@uci.edu (J.V. Jester).

1. Introduction

UVA-riboflavin induced corneal collagen crosslinking (UVA CXL) is a commonly used therapy for the treatment of corneal ectatic diseases such as keratoconus and post LASIK ectasia which weaken the corneal stroma leading to progressive, severe astigmatism. This technique, developed by Spoerl and Wollensak (Raiskup and Spoerl, 2013; Spoerl et al., 1998; Wollensak et al., 2003a), works when activation of riboflavin within the corneal stroma induces the production of oxygen free radicals which in turn induce covalent crosslinking of collagen fibrils (Kamaev et al., 2012; Raiskup and Spoerl, 2013). Induced crosslinking enhances blue collagen autofluorescence (CAF) and has been shown to produce a 2–3 fold increase in corneal elastic modulus, lasting increased stiffness in human corneas up to 300% (Bradford et al., 2016, 2017; Wollensak and Iomdina, 2009; Wollensak et al., 2003a), and at least one diopter of corneal flattening lasting a year or longer (De Bernardo et al., 2015; Elling et al., 2017; Hersh et al., 2017; Kanellopoulos and Asimellis, 2015; Malik et al., 2017; Raiskup-Wolf et al., 2008; Shalchi et al., 2015; Vinciguerra et al., 2009; Wollensak et al., 2003a).

This treatment has many known effects on corneal tissue, including a dose dependent cellular toxicity, corneal haze, collagen fiber thickening up to 12% within the crosslinked region, and possibly straightening of the collagen fibers (De Bernardo et al., 2015; Kanellopoulos and Asimellis, 2015; Malik et al., 2017; Shalchi et al., 2015; Wollensak et al., 2003a, 2004b). In particular, keratocytes and endothelial cells are both at risk of damage, and cell death occurs within the crosslinked volume (Kozobolis et al., 2016; Kruger et al., 2011; Wollensak et al., 2003b, 2007, 2004a). It has previously been observed that keratocyte repopulation begins around one month post crosslinking in rabbits (Kozobolis et al., 2016; Kruger et al., 2011; Wollensak et al., 2007), with full repopulation at six weeks. Wollensak (Wollensak et al., 2007) and Kozobolis (Kozobolis et al., 2016) both used light microscopy to observe keratocyte repopulation into the irradiated region. Wollensak reported full cellular activity by 6 weeks. Both reported a continuing presence of acellular areas and apoptotic changes such as apoptotic bodies, shrunken cell nuclei, and chromatin condensation at 4 weeks, especially around the periphery of irradiation. Kruger (Kruger et al., 2011) also observed cellular repopulation by 6 weeks using a combination of confocal laser scanning microscopy and two photon excited fluorescence, but observed a lower cellular density than seen in controls.

In addition to observing wound healing after crosslinking treatment, many previous studies have focused on changes to the collagen fibers and/or lamellae post treatment, particularly the waviness or crimping of the fibers and/or lamellae. Various measurements of collagen crimp in the cornea or sclera have been made, including waviness, fiber orientation, or branching point density, and methods for obtaining these measurements include a wide range of imaging techniques, including computational models, light microscopy, MRI, x-ray scattering, and many more (Grytz and Meschke, 2010; Ho et al., 2014; Kamma-Lorger et al., 2010; Kruger et al., 2011; Meek and Fullwood, 2001; Pierlot et al., 2014; Pijanka et al., 2012). In particular, SHG signals, which are the result of frequency doubling of near infrared irradiation through noncentrosymmetric materials, have been useful for imaging corneal collagen lamellar structure (Grytz and Meschke, 2010; Han et al., 2005; Ho et al., 2014;

Kamma-Lorger et al., 2010; Kruger et al., 2011; Meek and Fullwood, 2001; Mercatelli et al., 2017; Park et al., 2015; Pierlot et al., 2014; Pijanka et al., 2012; Quantock et al., 2015; Tan et al., 2013; Winkler et al., 2011; Zyablitskaya et al., 2017). This study is novel in that it examines the collagen crimp in specific regions of the cornea associated with enhanced collagen autofluorescence, a marker for collagen crosslinking.

The first objective of this study was to monitor in vivo changes after UVA CXL treatment. For this in vivo confocal microscopy through focus (CMTF) was used to monitor measurements of corneal thickness and haze during healing, and fluorescent staining was performed after sacrifice to observe cellular differences at one and three months after treatment. CMTF is a well-developed technology that has previously been used to monitor corneal wound healing in vivo (Li et al., 2000; Mazzotta et al., 2015; Moller-Pedersen et al., 1998). Another aim of this study was to measure degree of crimping in collagen after treatment. If corneal flattening is due to fiber shortening it would also lead to the straightening of fibers. SHG imaging was used to detect a decrease in fiber, i.e. lamellar, crimping. Finally, CAF was measured at both time points with the intention of assessing the persistence of collagen crosslinking and precisely locating regions of crosslinking within the cornea.

2. Methods

2.1. Animals

For this experiment two groups of four rabbits each, ages 3–9 months, were treated with standard UVA CXL in the right eye. All animals were treated according to the ARVO statement on the use of animals in vision research and experiments were approved by the IACUC of the University of California, Irvine. The first group consisted of 4 Dutch belted rabbits which were sacrificed one month after treatment. The second group consisted of 4 New Zealand albino rabbits sacrificed three months after treatment. In both cases the opposite eye of each animal was left untreated to be used as a control.

Prior to treatment, all rabbits were sedated with a subcutaneous injection of 30–50 mg/kg ketamine hydrochloride (Hospira, Irvine, CA) and 5–10 mg/kg xylazine (Akorn, Lake Forrest, IL) and images were taken of the right cornea using in vivo CMTF imaging to provide baseline measurements of epithelial and stromal thickness, and corneal haze.

2.2. UVA CXL

UVA CXL treatment was performed using a standard UVA CXL protocol (Raiskup-Wolf et al., 2008; Spoerl et al., 1998; Wollensak et al., 2003a). Rabbits were initially sedated using ketamine/xylazine, with additional sedation as needed. Each animal then received a drop of topical ophthalmic 0.5% tetracaine hydrochloride (Alcon, Ft. Worth, TX) to prevent pain during treatment. Using a lid speculum to keep the eye open, the central 8 mm of the right cornea was marked with an 8 mm diameter trephine. The epithelium was then removed from this region by gently scraping the surface with a Tooke knife. Next sterile photosensitizing solution comprising of 0.1% riboflavin-5-phosphate (Sigma-Aldrich, St. Louis, MO) solution in phosphate buffered saline (PBS: pH 7.2) containing 20% high-fraction dextran,

molecular weight 450–650 KDa (Sigma-Aldrich, St. Louis, MO) was applied to the stroma dropwise every two minutes for 30 min. Corneas were then exposed to 370 nm UVA light at 3 mW/cm^2 for 30 min with continued application of riboflavin solution every 2 min. After treatment, each rabbit received a drop of 0.3% gentamycin sulfate (Allergan, Inc., Irvine, CA) in the treated eye. Each rabbit was treated with gentamycin eye drops three times daily for three days post treatment to prevent infection.

2.3. In vivo imaging

After treatment rabbits were monitored during healing using CMTF imaging to measure changes in epithelial thickness, stromal thickness, and corneal haze using techniques previously reported (Li et al., 2000; Mazzotta et al., 2015; Moller-Pedersen et al., 1998). Briefly, a series of XY plane images through the entire depth of the cornea was captured and a 3D reconstruction of those images provided an in vivo cross sectional view of the healing cornea. A graph was then made for each image by plotting intensity versus depth. An increased area of intensity, or haze, can easily be seen within the cross sections of treated eyes. Peaks of intensity also represent natural structures such as the epithelium, the beginning of the stroma, and the endothelium. Epithelial and stromal thickness were calculated by measuring the distance between intensity peaks. A measure of haze was obtained by finding the area under the curve within the stroma.

Measurements were taken pre-operatively and at 2, 4, 8, and 12 weeks. All rabbits were sacrificed following their last CMTF measurements at 4 weeks (4 rabbits) and 12 weeks (4 rabbits) using a 1 ml injection of Euthanasia III (Vedco, Inc. St. Joseph, MO) into the marginal ear vein.

2.4. Imaging

Immediately after sacrifice eyes were perfusion fixed in situ at 20 mmHg using 2% paraformaldehyde (PFA, Mallinckrodit Baker, Inc., Phillipsburg, NJ) in PBS for 5 min to maintain the in vivo collagen structure. It has been previously shown that corneas fixed in this way do not exhibit any artifact as a result of the mechanical unloading of collagen fibers as the cornea is removed from the globe, or as a result of the fixation itself (Quantock et al., 2015). Corneas were then excised and left in PFA overnight at 4 °C. The cornea was then embedded in 10% low melting point agarose (Lonza, Rockland, ME) and cut into 250 μm thick cross sections, extending limbus to limbus, using a vibratome (Campden Instruments, Loughborough, England) and imaged with a Zeiss LSM 510 (Carl Zeiss, Jena, Germany).

Two photon excitation with 760 nm femtosecond laser light (Chameleon, Coherent Inc., Santa Clara, CA) was used to observe CAF, collected over a range of 400–450 nm, as previously described (Bradford et al., 2016, 2017; Chai et al., 2011). Since CAF is known to be enhanced by induced crosslinking (Chai et al., 2011), and to be correlated with increased mechanical stiffness (Bradford et al., 2016, 2017), it was used to locate the area of treatment and determine whether the stiffening effect had persisted over time. SHG images were then taken within the same sections, using two photon excitation at 820 nm, and collecting 390–465 nm, to observe the corneal collagen matrix, and to examine the crimping within the collagen structure. SHG imaging has often been used to study corneal collagen organization

(Han et al., 2005; Mercatelli et al., 2017; Park et al., 2015; Quantock et al., 2015; Tan et al., 2013; Winkler et al., 2011; Zyablitskaya et al., 2017). Image stacks, 100–200 μm deep and 427 μm wide, were taken in varying areas of each section using a 40× objective (1.3 NA), so as to cover the entire epithelial to endothelial thickness in each image. Four SHG image stacks were taken per treated cornea, two in the central cornea, and two in the untreated periphery, outside of the region showing CAF. One SHG image stack was taken per control cornea, in the central region. Finally, sections were stained with phalloidin [1:100] and propidium iodide (0.001 mg/ml) to label extracellular factin and DNA respectively. Fluorescent imaging was performed on stained sections using an excitation of 488 nm and collecting 500–550 nm and 565–615 nm for phalloidin and propidium iodide respectively to observe cellular differences between samples.

2.5. Image analysis

CAF was measured using previously reported methods (Bradford et al., 2016, 2017). Briefly, intensities were measured using Metamorph imaging software (Metamorph; Molecular Devices, Sunnyvale, CA). The average value in each image was measured within 6 different 100 by 100 pixel regions of interest, three placed within the crosslinked region and 3 placed in the background. Crosslinked region intensities were averaged together as were background intensities, and the two were subtracted from each other to yield one measurement of increased intensity due to crosslinking.

To quantify crimping of collagen, three planes within each SHG image stack were used for calculation. In each plane, the path of three fibers were traced across the entire width of the image using Metamorph in both the anterior and posterior stroma. A value for collagen fiber crimping (CFC) was calculated as a ratio of the length of the traced fiber to the length of a straight path in the same location. An example of this measurement is shown in Fig. 1. These values were calculated for the central treated region and periphery of each treated cornea as well as the central region of each control cornea.

2.6. Statistics

In all cases statistical analysis was performed using the Tukey-Kramer method for a multiple comparison, one-way analysis of variance (ANOVA) in Matlab (Mathworks, Natick, MA) with a P value of less than 0.05 considered statistically significant.

3. Results

3.1. CMTF

Measurements of epithelial thickness, stromal thickness, and haze over time are graphed in Fig. 2 and listed in Table 1. As shown in Fig. 2A, measurements of epithelial thickness over time remained consistent, showing no significant differences ($P > 0.6$) in either group. Stromal thickness (Fig. 2B) however did show significant changes. By 3 months, in group 2, it had surpassed its original baseline thickness of 301.5 ± 4.9 μm to 327.4 ± 8.2 μm, a change of 25.9 μm. While it was statistically significant, the increase was less than 10%, not likely clinically significant. In both groups haze (Fig. 2C) increased for the first month following treatment, the most significant increase measured at 2 weeks post treatment with a

5.5 fold and 3.1 fold increase in groups 1 and 2 respectively. In both groups haze peaked at one month, with values of 2277 ± 272 and 2168 ± 334.1 in arbitrary units (AU). It then began to decrease in group 2 to a final three month value of 1207 ± 126.7. This was significantly decreased from the one month peak, and was no longer significantly increased from baseline. The CMTF cross sectional views shown in Fig. 3 provide a visual representation of this change in haze over time.

As expected, examination of CMTF images also revealed an acellular zone in the anterior cornea. The increased intensity of the hazy region, shown in Fig. 3, followed this acellular region.

3.2. CAF

Representative CAF images from one and three months post CXL are shown in Fig. 4. CAF averaged 1267 ± 181 AU at one month and 1224.2 ± 158 AU at three months in the two separate groups which was not significantly different. There was also no significant difference between the depths of crosslinking in either group, measuring 42.4 ± 3.4% and 47.7 ± 7.6% of the total thickness.

3.3. Collagen crimping

Fig. 5 shows representative images of each region used to measure crimp in both one (A, C, E) and three (B, D, F) month samples. CFC values calculated for each region are shown in Table 2. At one month, the crosslinked region showed a significantly decreased measure of crimp compared to all other regions. In the anterior of the control sample (E), crimp measured 1.017 ± 0.004, that is, 1.7% longer than a straight path. When looking at the anterior of the central region of the one month treated cornea (A), crimp measured 1.0067 ± 0.0058, which is significantly straighter compared to control ($P < 0.05$). In the periphery of treated eyes, outside of the region of CXL, crimping was 1.017 ± 0.0013 (not shown), no different than the control (E and F). Also, no significant difference was detected between any values in the posterior stroma. Similarly, at three months, the anterior region of the CXL cornea was the only region with significantly lower crimp measurements, averaging 1.009 ± 0.0049 (C), which was not significantly different from one month.

3.4. Cellular repopulation

Although confocal images showed a significant reduction in haze from one to three months, staining with phalloidin and PI showed incomplete repopulation of cells into the acellular zone of the central cornea, seen in Fig. 6A (1 month) and 6C (3 months). Images taken in the central cornea show almost no repopulation at either time point, indicated by the lack of keratocytes in the region of CAF, shown in blue. Additionally, the depth of the acellular region is not significantly different than the depth of CAF at both time points, 40.5 ± 4.1% versus 42.4 ± 3.4% at one month and 43.7 ± 11.3% versus 47.7 ± 7.6% at three. This is also in agreement with CMTF images taken within the treatment region, which show no cells anterior to the region of haze at all time points. In the periphery, however, cellular migration into the area of CXL was observed at one month, which appeared greater at three months, Fig. 6B and D.

These images also yielded an unexpected result. As shown in Fig. 6A, one month samples appeared to have a loss of keratocytes in the posterior, un-crosslinked region. In two of the four samples this area was almost entirely acellular. Three month samples showed a more uniform cellular distribution below the crosslinked region, Fig. 6C.

4. Discussion

CMTF imaging was used in this study to monitor the changes in epithelial thickness, stromal thickness, and haze over time after crosslinking treatment. Little change was detected in epithelial or stromal thickness, but a large change was detected in corneal haze during healing. This is in agreement with the temporary haze others have observed clinically (Hersh et al., 2017). Stromal thickness did show a slight but steady increase over time, which was only significantly different after the full three months. This was likely not a result of the crosslinking procedure itself, but of the natural aging of the animal. It has been shown that the central thickness of rabbit corneas increases steadily with increasing age at a rate consistent to that seen in this study, about 25 μm in a three month period. (Doughty, 1994).

Fluorescent cellular staining on corneal sections provided a better view of the cellular differences between one and three month samples. Contrary to previous reports, which indicated cellular repopulation after 4–6 weeks of recovery in rabbits (Kozobolis et al., 2016; Kruger et al., 2011; Wollensak et al., 2007), cellular repopulation was only observed in the peripheral cornea, around the edges of the CXL area. This was shown both visually in the images and quantitatively when CAF depth was compared to cell depth, and no difference was found. Images taken at the edge of the treated region did show more cells which overlapped the blue CAF at one month, Fig. 6B, and even more at three months, Fig. 6D. This indicates that cells are migrating in from the periphery, consistent with previous reports (Kozobolis et al., 2016; Wollensak et al., 2007). Contrary to these reports, however, cellular repopulation was not fully completed after three months. The current study is more consistent with the results from Kruger (Kruger et al., 2011), who reported cellular migration beginning as early as 3 days and repopulation at 6 weeks which still lacked the full cellular density of controls. The authors of that report cited the youth of the rabbits used as an explanation for earlier repopulation than expected. Also observed in the stained sections was a region of fewer or no cells at one month in the posterior central cornea, outside the area of CAF, Fig. 6A. This finding was not detected by the in vivo CMTF imaging, possibly because of the lower resolution of that technique. This is in agreement with literature (Kozobolis et al., 2016) but more work needs to be done to identify a possible cause.

It should also be noted that no change in CAF was observed between 1 month and 3 months after crosslinking. Previous studies have linked changes in CAF to changes in stiffening using both mechanical indentation testing and enzymatic digestion (Bradford et al., 2016, 2017; Chai et al., 2011). Therefore the finding that CAF is not changed over time suggests that the stiffening effect may also persist for at least three months. This is in agreement with mechanical studies, which have also shown a persistence in the stiffening effect, and with clinical studies which show a lasting visual improvement (Hersh et al., 2017; Wollensak and Iomdina, 2009).

Lastly, many groups have studied the changes in corneal collagen and corneal shape following UVA CXL with clinical studies showing a significant reduction in corneal curvature (De Bernardo et al., 2015; Elling et al., 2017; Hersh et al., 2017; Kanellopoulos and Asimellis, 2015; Malik et al., 2017; Shalchi et al., 2015; Wollensak et al., 2003a). This study identified a significant reduction of collagen crimping following UVA CXL in vivo, a change which persisted over time, and was present only within the treatment region as identified by CAF. There are at least three plausible explanations for this observation. 1) Reduction in collagen crimp could be due to the resistance of relaxation of crosslinked fibers or an artifact of fixation, 2) Straightening of fibers is due to corneal edema, or 3) Collagen straightening is due to collagen fiber shortening.

The first explanation of our collagen crimping observations assumes that the treated area, being mechanically stiffer than surrounding tissue, does not relax in the same manner when the cornea is excised. This would cause skewed crimping comparisons. The corneas in this study, however, were fixed under pressure to avoid this artifact, which has previously been shown to be effective (Quantock et al., 2015). Also, it is worth noting that crimping due to any other fixation artifact would likely have affected the whole tissue, not just the periphery.

The second explanation assumes that a swollen cornea should have straighter fibers. There are several observations indicating that this may not be the case. For example, clinical results show a wide range of both increasing and decreasing corneal thicknesses after treatment, while still showing a trend of reduced corneal curvature (Shalchi et al., 2015). This suggests that the cause of fiber straightening is more complex than just edema. Moreover, since the corneal thickening seen in this study did not occur immediately after treatment, but gradually over time and was consistent with observations of age related changes in corneal thickness of rabbits in the literature (Doughty, 1994), we believe that the increase in thickness observed in this study was not edema caused by treatment but was instead a natural aging process. More specifically, if the increase in thickness was due to edema that caused decreased collagen fiber crimping, then we should have observed significantly less crimping at 3 months compared to 1 month after crosslinking, which was not the case. It has also been shown that when swelling does occur in the corneal stroma, it happens predominantly in the posterior, leaving the anterior structure unchanged (Muller et al., 2001). Swelling was also noted by Muller et al. to cause increased waviness of the collagen lamellae, which would result in increased crimp, not decreased crimp. Finally, there is also evidence in the literature showing that collagen crosslinking reduces the swelling pressure within the treatment region, making it unlikely that crosslinking induces edema in the region of treatment (Sondergaard et al., 2013).

The final explanation is that collagen straightening, and corneal flattening could be due to fiber shortening. If fibers are shorter after crosslinking, it would be logical that they would also be straighter. If the arc length across the cornea is the same or reduced after the procedure, and the fiber length were to remain constant, then a region of straightened fibers would have to result in increased crimp outside of the treatment region. In other words, the fiber would have to go somewhere. This study showed no change in crimp in any of the surrounding regions. This observation, combined with the evidence listed against the first two explanations leads us to believe this is the most plausible of the three explanations.

Furthermore, other studies have observed changes in the extracellular matrix, including increased collagen fibril diameter and decreased interfibrillar spacing, all of which could be associated with collagen fibril shortening (Kruger et al., 2011; Tan et al., 2013; Wollensak et al., 2004b). It is unlikely that all these changes are independent of one another, and therefore it is likely that they all play some role, directly or indirectly, to affect corneal curvature. Certainly, more studies are needed to fully understand the effects of UVA CXL on corneal collagen structure and corneal shape.

5. Conclusions

Results from in vivo CMTF imaging post UVA CXL showed relatively consistent values of epithelial and stromal thickness over time, and a trend in corneal haze which peaked at one month and then decreased. After sacrifice, various imaging methods were used to determine differences between one and three months of recovery. There was no difference in CAF between the two time points. SHG images of collagen fibers were used to detect a decrease in collagen crimp following UVA CXL treatment. Also, cellular staining showed cellular migration only into the periphery of the treated region.

Acknowledgements

National Eye Institute (NEI), and Research to Prevent Blindness (RPB), Inc.

Funding

Supported by NEI EY024600.

References

Bradford SM, Brown DJ, Juhasz T, Mikula E, Jester JV, 2016 Nonlinear optical corneal collagen crosslinking of ex vivo rabbit eyes. J. Cataract Refract. Surg 42, 1660–1665. [PubMed: 27956294]

Bradford SM, Mikula ER, Chai D, Brown DJ, Juhasz T, Jester JV, 2017 Custom built nonlinear optical crosslinking (NLO CXL) device capable of producing mechanical stiffening in ex vivo rabbit corneas. Biomed. Optic Express 8, 4788–4797.

Chai D, Gaster RN, Roizenblatt R, Juhasz T, Brown DJ, Jester JV, 2011 Quantitative assessment of UVA-riboflavin corneal cross-linking using nonlinear optical microscopy. Invest. Ophthalmol. Vis. Sci 52, 4231–4238. [PubMed: 21508101]

De Bernardo M, Capasso L, Lanza M, Tortori A, Iaccarino S, Cennamo M, Borrelli M, Rosa N, 2015 Long-term results of corneal collagen crosslinking for progressive keratoconus. J Optom 8, 180–186. [PubMed: 26105541]

Doughty MJ, 1994 The cornea and corneal endothelium in the aged rabbit. Optom. Vis. Sci 71, 809–818. [PubMed: 7898890]

Elling M, Kersten-Gomez I, Dick HB, 2017 Photorefractive intrastromal corneal crosslinking for the treatment of myopic refractive errors: six-month interim findings. J. Cataract Refract. Surg 43, 789–795. [PubMed: 28732613]

Grytz R, Meschke G, 2010 A computational remodeling approach to predict the physiological architecture of the collagen fibril network in corneo-scleral shells. Biomechanics Model. Mechanobiol 9, 225–235.

Han M, Giese G, Bille J, 2005 Second harmonic generation imaging of collagen fibrils in cornea and sclera. Optic Express 13, 5791–5797.

Hersh PS, Stulting RD, Muller D, Durrie DS, Rajpal RK, 2017 United States multicenter clinical trial of corneal collagen crosslinking for keratoconus treatment. Ophthalmology 124 (10), 1475–1484. [PubMed: 28655538]

Ho LC, Sigal IA, Jan NJ, Squires A, Tse Z, Wu EX, Kim SG, Schuman JS, Chan KC, 2014 Magic angle-enhanced MRI of fibrous microstructures in sclera and cornea with and without intraocular pressure loading. Invest. Ophthalmol. Vis. Sci 55, 5662–5672. [PubMed: 25103267]

Kamaev P, Friedman MD, Sherr E, Muller D, 2012 Photochemical kinetics of corneal cross-linking with riboflavin. Invest. Ophthalmol. Vis. Sci 53, 2360–2367. [PubMed: 22427580]

Kamma-Lorger CS, Boote C, Hayes S, Moger J, Burghammer M, Knupp C, Quantock AJ, Sorensen T, Di Cola E, White N, Young RD, Meek KM, 2010 Collagen and mature elastic fibre organisation as a function of depth in the human cornea and limbus. J. Struct. Biol 169, 424–430. [PubMed: 19914381]

Kanellopoulos AJ, Asimellis G, 2015 Combined laser in situ keratomileusis and pro-phylactic high-fluence corneal collagen crosslinking for high myopia: two-year safety and efficacy. J. Cataract Refract. Surg 41, 1426–1433. [PubMed: 26287881]

Kozobolis V, Gkika M, Sideroudi H, Tsaragli E, Lydataki S, Naoumidi I, Giatromanolaki A, Mikropoulos D, Teus M, Labiris G, 2016 Effect of riboflavin/UVA collagen cross-linking on central cornea, limbus and intraocular pressure. Experimental study in rabbit eyes. Acta Med. 59, 91–96.

Kruger A, Hovakimyan M, Ramirez Ojeda DF, Stachs O, Wree A, Guthoff RF, Heisterkamp A, 2011 Combined nonlinear and femtosecond confocal laser-scanning microscopy of rabbit corneas after photochemical cross-linking. Invest. Ophthalmol. Vis. Sci 52, 4247–4255. [PubMed: 21498616]

Li J, Jester JV, Cavanagh HD, Black TD, Petroll WM, 2000 On-line 3-dimensional confocal imaging in vivo. Invest. Ophthalmol. Vis. Sci 41, 2945–2953. [PubMed: 10967049]

Malik S, Humayun S, Nayyar S, Ishaq M, 2017 Determining the efficacy of corneal crosslinking in progressive keratoconus. Pak J Med Sci 33, 389–392. [PubMed: 28523043]

Mazzotta C, Hafezi F, Kymionis G, Caragiuli S, Jacob S, Traversi C, Barabino S, Randleman JB, 2015 In vivo confocal microscopy after corneal collagen crosslinking. Ocul. Surf 13, 298–314. [PubMed: 26142059]

Meek KM, Fullwood NJ, 2001 Corneal and scleral collagens–a microscopist's perspective. Micron 32, 261–272. [PubMed: 11006506]

Mercatelli R, Ratto F, Rossi F, Tatini F, Menabuoni L, Malandrini A, Nicoletti R, Pini R, Pavone FS, Cicchi R, 2017 Three-dimensional mapping of the orientation of collagen corneal lamellae in healthy and keratoconic human corneas using SHG microscopy. J. Biophot 10, 75–83.

Moller-Pedersen T, Li HF, Petroll WM, Cavanagh HD, Jester JV, 1998 Confocal microscopic characterization of wound repair after photorefractive keratectomy. Invest. Ophthalmol. Vis. Sci 39, 487–501. [PubMed: 9501858]

Muller LJ, Pels E, Vrensen GF, 2001 The specific architecture of the anterior stroma accounts for maintenance of corneal curvature. Br. J. Ophthalmol 85, 437–443. [PubMed: 11264134]

Park CY, Lee JK, Chuck RS, 2015 Second harmonic generation imaging analysis of collagen arrangement in human cornea. Invest. Ophthalmol. Vis. Sci 56, 5622–5629. [PubMed: 26313297]

Pierlot CM, Lee JM, Amini R, Sacks MS, Wells SM, 2014 Pregnancy-induced remodeling of collagen architecture and content in the mitral valve. Ann. Biomed. Eng 42, 2058–2071. [PubMed: 25103603]

Pijanka JK, Coudrillier B, Ziegler K, Sorensen T, Meek KM, Nguyen TD, Quigley HA, Boote C, 2012 Quantitative mapping of collagen fiber orientation in non-glaucoma and glaucoma posterior human sclerae. Invest. Ophthalmol. Vis. Sci 53, 5258–5270. [PubMed: 22786908]

Quantock AJ, Winkler M, Parfitt GJ, Young RD, Brown DJ, Boote C, Jester JV, 2015 From nano to macro: studying the hierarchical structure of the corneal extracellular matrix. Exp. Eye Res. 133, 81–99. [PubMed: 25819457]

Raiskup-Wolf F, Hoyer A, Spoerl E, Pillunat LE, 2008 Collagen crosslinking with riboflavin and ultraviolet-A light in keratoconus: long-term results. J. Cataract Refract. Surg 34, 796–801. [PubMed: 18471635]

Raiskup F, Spoerl E, 2013 Corneal crosslinking with riboflavin and ultraviolet A. I. Principles. Ocul. Surf 11, 65–74. [PubMed: 23583042]

Shalchi Z, Wang X, Nanavaty MA, 2015 Safety and efficacy of epithelium removal and transepithelial corneal collagen crosslinking for keratoconus. Eye 29, 15–29. [PubMed: 25277300]

Sondergaard AP, Ivarsen A, Hjortdal J, 2013 Reduction of stromal swelling pressure after UVA-riboflavin cross-linking. Invest. Ophthalmol. Vis. Sci 54, 1625–1634. [PubMed: 23385796]

Spoerl E, Huhle M, Seiler T, 1998 Induction of cross-links in corneal tissue. Exp. Eye Res. 66, 97–103. [PubMed: 9533835]

Tan HY, Chang YL, Lo W, Hsueh CM, Chen WL, Ghazaryan AA, Hu PS, Young TH, Chen SJ, Dong CY, 2013 Characterizing the morphologic changes in collagen crosslinked-treated corneas by Fourier transform-second harmonic generation imaging. J. Cataract Refract. Surg 39, 779–788. [PubMed: 23608570]

Vinciguerra P, Albe E, Trazza S, Seiler T, Epstein D, 2009 Intraoperative and postoperative effects of corneal collagen cross-linking on progressive keratoconus. Arch. Ophthalmol 127, 1258–1265. [PubMed: 19822840]

Winkler M, Chai D, Kriling S, Nien CJ, Brown DJ, Jester B, Juhasz T, Jester JV, 2011 Nonlinear optical macroscopic assessment of 3-D corneal collagen organization and axial biomechanics. Invest. Ophthalmol. Vis. Sci 52, 8818–8827. [PubMed: 22003117]

Wollensak G, Iomdina E, 2009 Long-term biomechanical properties of rabbit cornea after photodynamic collagen crosslinking. Acta Ophthalmol. 87, 48–51. [PubMed: 18547280]

Wollensak G, Iomdina E, Dittert DD, Herbst H, 2007 Wound healing in the rabbit cornea after corneal collagen cross-linking with riboflavin and UVA. Cornea 26, 600–605. [PubMed: 17525659]

Wollensak G, Spoerl E, Seiler T, 2003a Riboflavin/ultraviolet-a-induced collagen crosslinking for the treatment of keratoconus. Am. J. Ophthalmol 135, 620–627. [PubMed: 12719068]

Wollensak G, Spoerl E, Wilsch M, Seiler T, 2003b Endothelial cell damage after riboflavin-ultraviolet-A treatment in the rabbit. J. Cataract Refract. Surg 29, 1786–1790. [PubMed: 14522302]

Wollensak G, Spoerl E, Wilsch M, Seiler T, 2004a Keratocyte apoptosis after corneal collagen cross-linking using riboflavin/UVA treatment. Cornea 23, 43–49. [PubMed: 14701957]

Wollensak G, Wilsch M, Spoerl E, Seiler T, 2004b Collagen fiber diameter in the rabbit cornea after collagen crosslinking by riboflavin/UVA. Cornea 23, 503–507. [PubMed: 15220736]

Zyablitskaya M, Takaoka A, Munteanu EL, Nagasaki T, Trokel SL, Paik DC, 2017 Evaluation of therapeutic tissue crosslinking (TXL) for myopia using second harmonic generation signal microscopy in rabbit sclera. Invest. Ophthalmol. Vis. Sci 58, 21–29. [PubMed: 28055099]

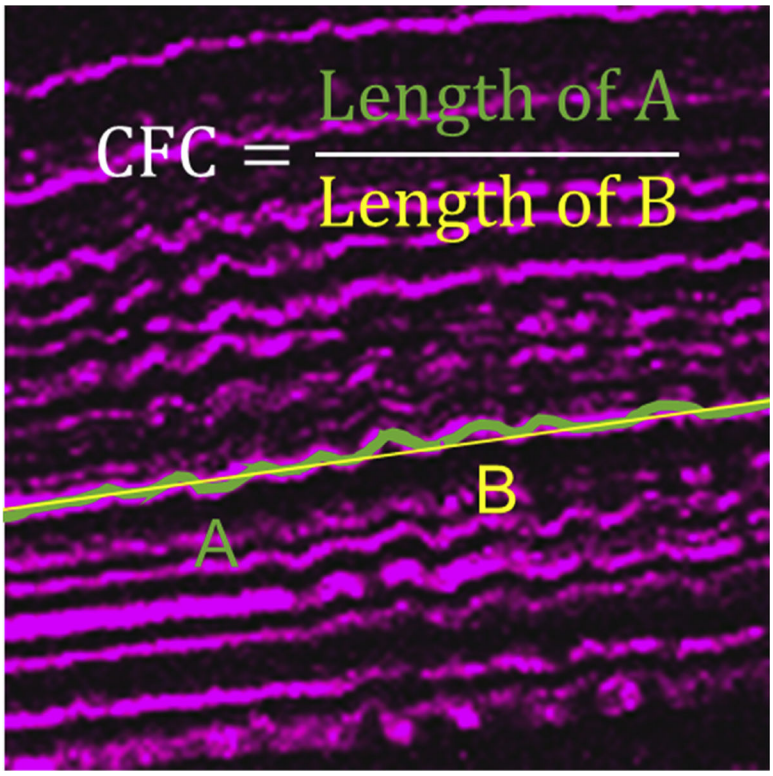

Fig. 1. Calculation of CFC.

CFC was calculated as the path length of a collagen fiber (A) divided by the length of a straight line through the same space (B).

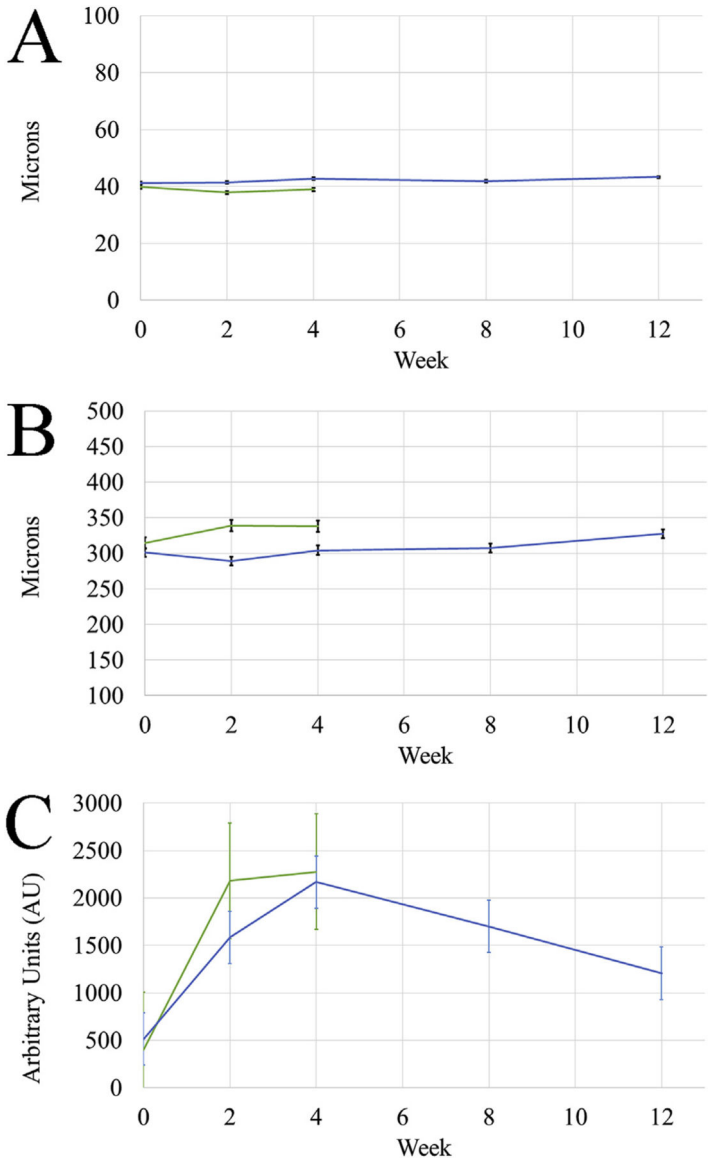

Fig. 2. In vivo CMTF Measurements.

Changes in epithelial and stromal thickness for both groups were measured over time. Plots of these measurements are shown in A and B respectively, with week 0 referring to initial baseline measurements prior to treatment and all other time points referring to the number of weeks after treatment. Both thickness measurements remained relatively constant, with only the three month stromal thickness being significantly different from initial values. Graph C shows the haze measured in arbitrary units at each time point throughout recovery, calculated as the area under the curve of a plot of intensity through the depth of the cornea. In both groups haze peaked at one month and then began to decrease in group 2.

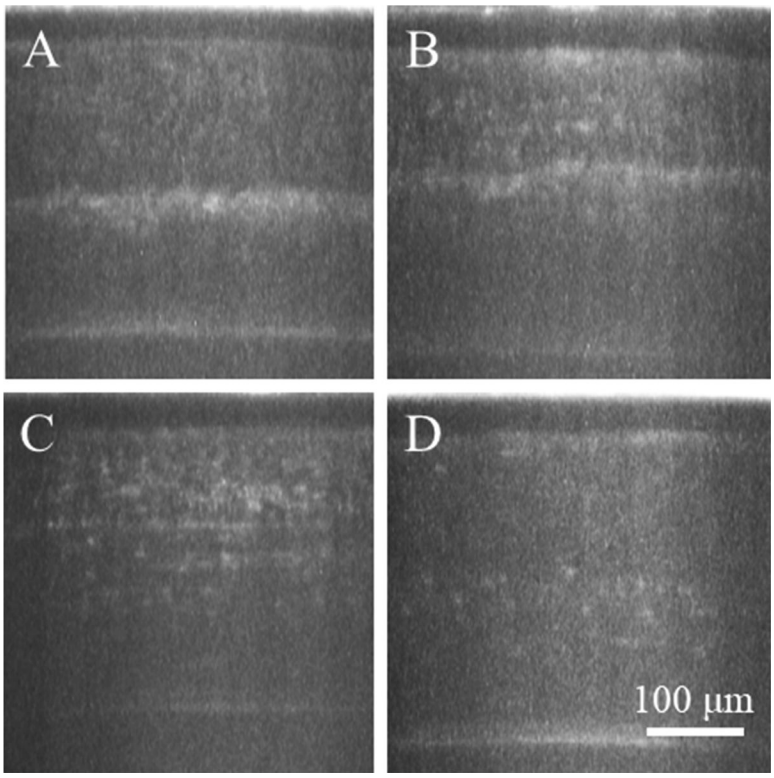

Fig. 3. Cross Sectional CMTF Images.

A visual representation of haze at each week is provided in the images, corresponding to 2 (A), 4 (B), 8 (C), and 12 (D) weeks post treatment. Each image is a cross sectional projection of the through focus images taken at each time point. At the two week time point (A), most of the haze is concentrated to the area just below the treated region. Throughout recovery (B–D) haze spreads, peaking in intensity at one month (B), and then decreases.

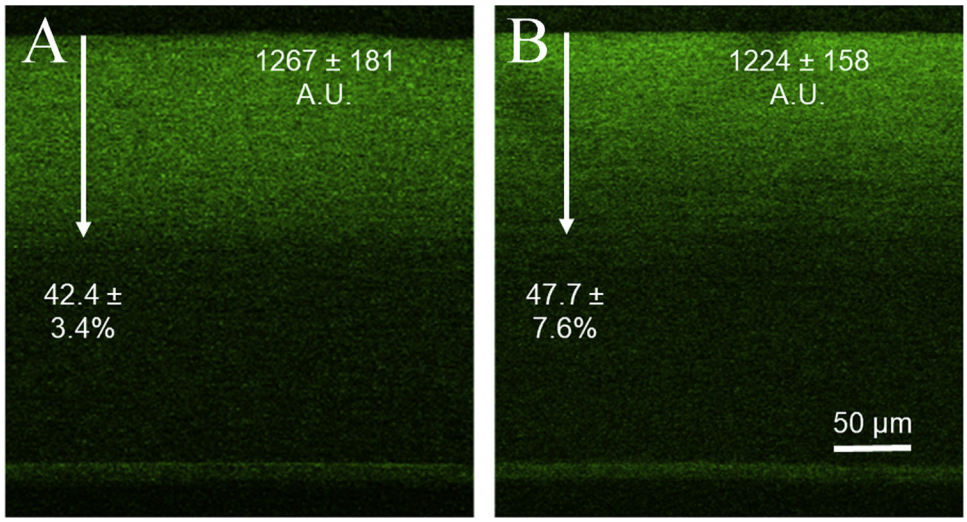

Fig. 4. Collagen Autofluorescence after 1 and 3 months.

The image in A is a CAF image taken within the central region of a one month sample. The average intensity increase in these samples was 1267 ± 181. The depth of crosslinking, measured by depth of increased intensity and demonstrated with an arrow in the image, was found to be 42.4 ± 3.4% of the total stromal thickness on average at one month. The image in B shows the corresponding CAF image for the three month samples. CAF intensity and depth remained constant between the two time points with values of 1224 ± 158 and 47.7 ± 7.6% at three months.

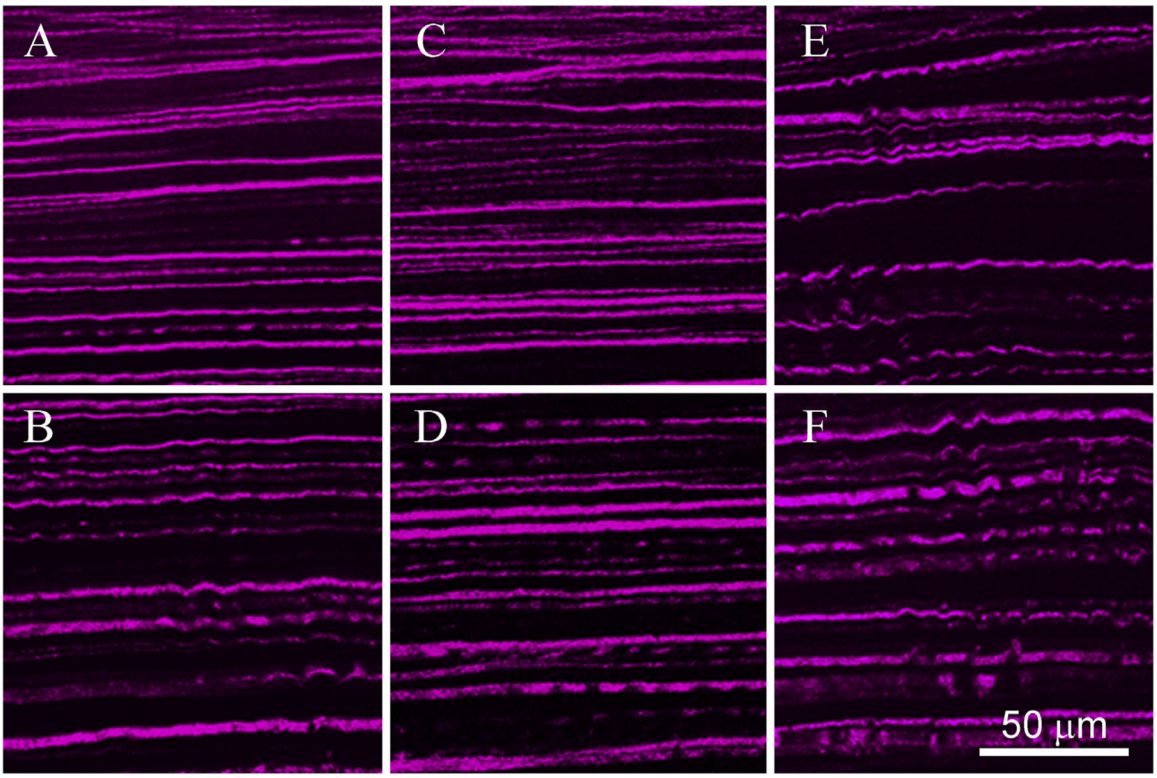

Fig. 5. SHG Images of Collagen Crimping.

Cross sectional SHG imaging revealed significantly straighter collagen fibers in the anterior of treated corneas at both one and three months (A and C respectively) when compared to their own posterior values (B and D) or control anterior or posterior values (E and F). Fibers were visibly wavier in all non-treated areas (B, D, E, and F).

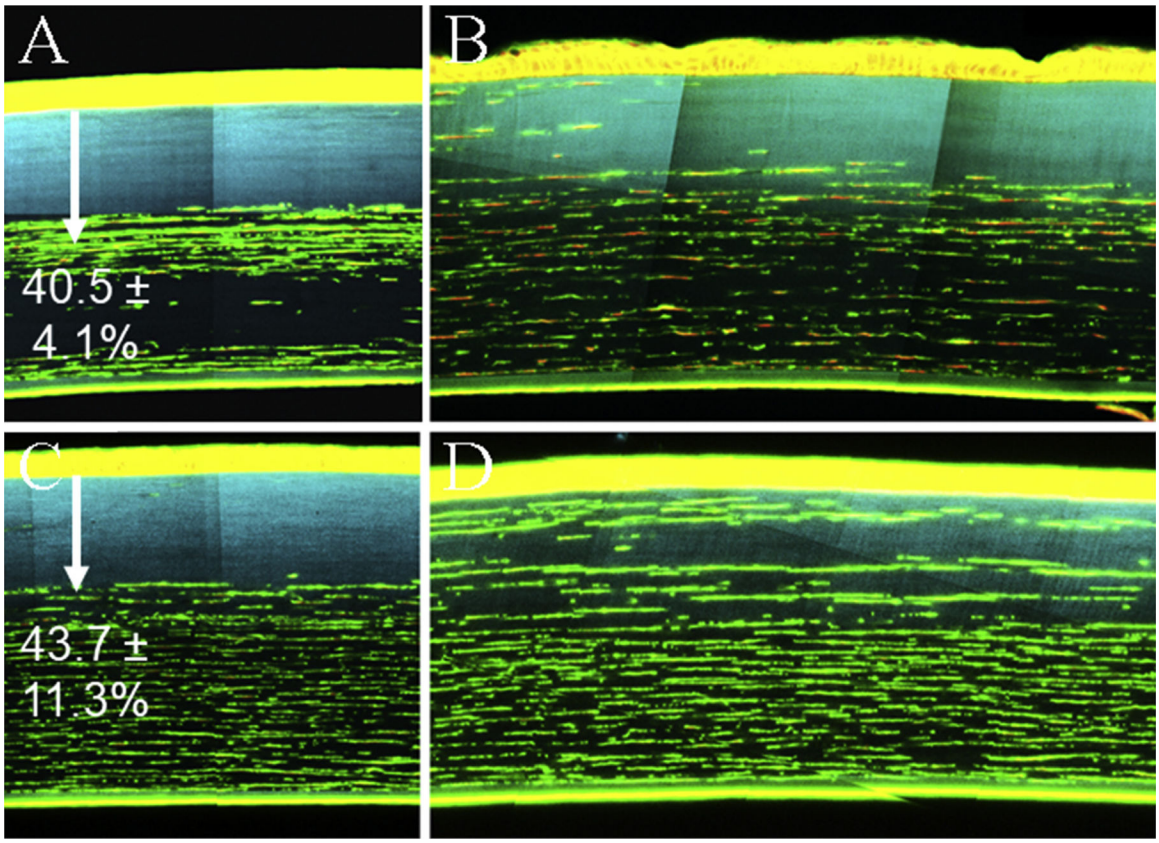

Fig. 6. Cell Staining.

The top row of images represents samples from the central CXL region and the edge of the CXL region bordering the periphery from one month samples (A and B respectively). The bottom row represents corresponding images from three month samples (C and D). Staining with Phalloidin (green; 1:100) and Propidium Iodide (red; 0.01 mg/ml) showed little cellular repopulation into the central CXL region, shown with blue CAF, at either time point. Images from the periphery show migrating cells into the CXL region. The depth of the acellular zone in the central cornea, indicated by arrows, was measured to be 40.5 ± 4.1%, and 43.7 ± 11.3% of the stromal thickness on average for one and three month samples. This corresponds to the measured depth of CAF. Also, in two of the four one month samples, a second deeper acellular region was noted, pictured in A. (For interpretation of the references to colour in this figure legend, the reader is referred to the Web version of this article.)

Table 1

Epithelial thickness, stromal thickness, and haze.

Week	Epithelial Thickness		Stromal Thickness		Haze	
	1 Month	3 Month	1 Month	3 Month	1 Month	3 Month
0	39.9 ± 0.5	41.2 ± 1.4	314.5 ± 15	301.5 ± 4.9	399.5 ± 55.1	514.6 ± 75.7
2	37.8 ± 0.9	41.4 ± 1.9	338.8 ± 3.5	288.8 ± 9.1	*2180 ± 333	*1585 ± 236
4	38.9 ± 1.7	42.7 ± 0.9	337.9 ± 8.7	304.4 ± 8.6	*2277 ± 272	*2168 ± 334
8	NA	41.8 ± 0.6	NA	307.3 ± 6.9	NA	*1700 ± 254
12	NA	43.3 ± 0.6	NA	*327.4 ± 8.2	NA	1207 ± 127

*P < 0.05 compared to Week 0.

Table 2

Collagen fiber crimp data.

Treatment	Time	Central		Peripheral	
		Anterior	Posterior	Anterior	Posterior
UVA CXL	1 Month	*1.007 ± 0.006	1.016 ± 0.004	1.017 ± 0.01	1.019 ± 0.07
	3 Month	*1.009 ± 0.005	1.022 ± 0.008	1.019 ± 0.06	1.019 ± 0.06
Control	1 Month	1.017 ± 0.04	1.022 ± 0.05	NA	NA
	3 Month	1.016 ± 0.06	1.024 ± 0.08	NA	NA

*P < 0.05 compared to corresponding posterior or control values.